Bioorganic Chemistry 103 (2020) 104108

Contents lists available at ScienceDirect

Bioorganic Chemistry

journal homepage: www.elsevier.com/locate/bioorg

Coumaric acid derivatives as tyrosinase inhibitors: Efficacy studies through *in silico*, *in vitro* and *ex vivo* approaches

Marina Themoteo Varela[a,1], Márcio Ferrarini[a,1], Vitória Gallo Mercaldi[a], Bianca da Silva Sufi[b], Giovana Padovani[b], Lucas Idacir Sbrugnera Nazato[b], João Paulo S. Fernandes[a,*]

[a] Department of Pharmaceutical Sciences, Institute of Environmental, Chemical and Pharmaceutical Sciences, Universidade Federal de São Paulo, Rua São Nicolau 210, 09913-030 Diadema-SP, Brazil
[b] Research and Development Department, Chemyunion Química Ltda, Av. Independência 1501, 18087-101 Sorocaba-SP, Brazil

ARTICLE INFO

Keywords:
Coumaric acid ester
Tyrosinase inhibitor
Antimelanogenic agent
Melanin synthesis inhibitor
Molecular docking

ABSTRACT

p-Coumaric acid is a known inhibitor of tyrosinase, an enzyme involved in the initial steps of the melanin synthesis in human and other species. However, its low lipophilicity impairs its penetration through skin and efficacy as antimelanogenic agent indeed. Accordingly, this paper reports the assessment of several coumaric acid derivatives as tyrosinase inhibitors and antimelanogenic agents in *in vitro*, *in silico* and *ex vivo* assays. The compounds were designed with modifications in the aromatic and acid moieties of *p*-coumaric acid, being the coumarate esters the most promising derivatives. The compounds showed higher tyrosinase inhibitory activity (pIC_{50} 3.7–4.2) than the parent acid, being compounds **1d**, **1e** and **1f** the most potent inhibitors. Docking analysis showed that these esters are competitive inhibitors *per se*, and act independently of a redox mechanism as suggested by DPPH assays. Moreover, the esters showed efficacy in reducing the melanin deposition in human skin fragments at 0.1% concentration, especially compound **1e**. In summary, there is an important equilibria between tyrosinase affinity and lipophilicity that must be considered to get effective antimelanogenic agents with adequate permeability in the skin.

1. Introduction

Melanin biosynthesis is a natural process that occurs in several living species, including plants, fungi and mammals. The limiting step in melanogenesis is controlled by metalloprotein tyrosinase, a copper-containing polyphenol oxidase that oxidizes L-tyrosine and L-DOPA into DOPA-quinone (Fig. 1) [1]. The biological importance of melanin is variable in each organism, but are mostly related to photoprotection from UV light and pigmentation. In humans, melanin is responsible for the different eye, hair and skin colors, as well as neural pigmentation, associated with neuromelanin [2].

Many dysfunctions and pathologies may come as a result of the excess or lacking melanin pigments produced in the cells. Albinism is a genetic disorder that is characterized by alteration of *TYR* gene, responsible for controlling the presence of tyrosinase in cells [3]. This alteration causes cells to be unable to produce melanin, giving to the individuals the characteristic pale skin and pink/red eyes and white hair. Excessive production of melanin is usually caused by prolonged and continuous sun exposure and also after inflammation processes in the skin, such as acne [4].

Tyrosinase is an enzyme present in several organisms, including plant, fungal and animal species, but with marked differences among them. For instance, human tyrosinase is an intracellular membrane-bound glycoprotein [5], while fungal tyrosinase is a soluble enzyme. Although the tyrosinases from different species differ considerably regarding several aspects of the protein structure, they share in common a similar active site, comprised by two copper atoms coordinated by three histidine residues, which catalyzes the oxidation reaction of phenols [6,7].

Mushroom tyrosinase is a widely used model for identifying tyrosinase inhibitors for human applications, since it is an accessible, commercially available enzyme due to its soluble characteristic [8,9]. Moreover, known inhibitors of mushroom tyrosinase usually exhibit increased potency in murine and human tyrosinases, and thus by identifying novel inhibitors in mushroom tyrosinase model, really effective antimelanogenic compounds may be expected [10,11].

There are many applications of melanin biosynthesis inhibitors in both pharmacological and cosmetic aspects, especially to treat

* Corresponding author at: Department of Pharmaceutical Sciences, Universidade Federal de São Paulo, Rua São Nicolau 210, 09913-030 Diadema-SP, Brazil.
E-mail address: joao.fernandes@unifesp.br (J.P.S. Fernandes).
[1] These authors contributed equally.

https://doi.org/10.1016/j.bioorg.2020.104108
Received 11 May 2020; Received in revised form 23 May 2020; Accepted 15 July 2020
Available online 21 July 2020

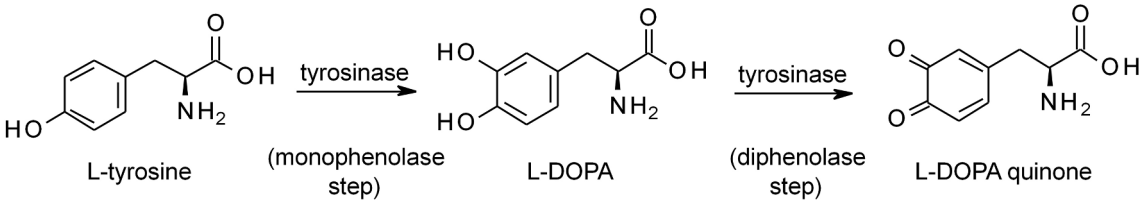

Fig. 1. Oxidation of the amino acid L-tyrosine to L-DOPA and then to DOPA-quinone.

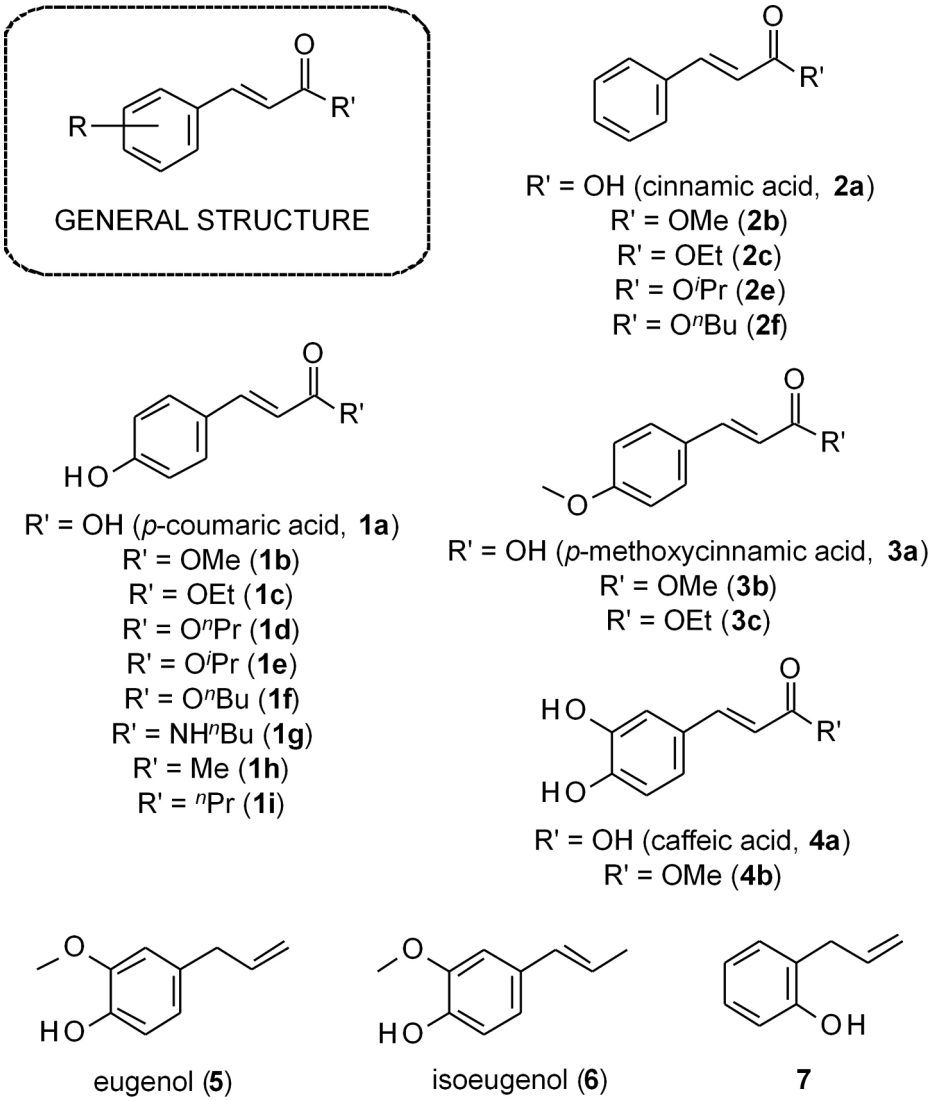

Fig. 2. Tested compounds.

dermatological hyperpigmentation. Natural products were historically used as drugs and drug prototypes [12] and the literature brings that *p*-coumaric acid is a natural inhibitor of tyrosinases [8,10,11]. *p*-Coumaric acid is a phenolic phenylpropanoid acid that have shown inhibitory activity on mushroom and human tyrosinases, as described in recent literature, which presents evident structural similarities with the tyrosinase substrate, the amino acid L-tyrosine [10,11]. Curiously, both phenylalanine and tyrosine are also substrates to the biosynthetic pathway of *p*-coumaric acid [13]. These considerable facts may explain the reason why *p*-coumaric acid can bind to the tyrosinases and inhibit their activities on melanin synthesis.

Although *p*-coumaric acid has inhibitory activity on tyrosinase, its poor penetration in the skin limited its application as antimelanogenic compound *in vivo*. To overcome this issue, its methyl ester was already evaluated as tyrosinase inhibitor [8], and showed to be more potent than the parent acid. However, limited information about other coumaric acid derivatives is reported in literature. Regarding this, the objective of the present study was to assess the activity of a set of coumaric acid analogues as antimelanogenic compounds, which considered a possible better penetration in the skin in the molecule's design. For this purpose, the inhibitory activity of several derivatives on mushroom tyrosinase through experimental and *in silico* assays (molecular docking) were performed, and *ex vivo* studies on human skin fragments for evaluating the efficacy as antimelanogenic agent were also done.

2. Material and methods

2.1. Chemicals and equipment

The chemicals were acquired from Sigma-Aldrich Co. in adequate purity to use in the experiments. The *p*-coumaric (**1a**), cinnamic (**2a**), *p*-methoxycinnamic (**3a**) and caffeic (**4a**) acids were used as starting materials for preparing the derivatives described below as well in the activity assays. Eugenol (**5**), isoeugenol (**6**) and 2-allylphenol (**7**) were also tested as acquired from commercial source. The mushroom tyrosinase (> 1000 U) solution was prepared in accordance to the manufacturer's instructions. The compounds were characterized through ^{1}H NMR spectroscopy in a Bruker Advance 300 spectrometer, operating at 300 MHz frequency, using TMS as internal standard and the chemical shifts (δ) are presented in ppm. The NMR data are in accordance to previous literature reports [14–21,47]. The purity of the compounds was chromatographically assessed through GC-MS in a Shimadzu QP2010 equipment and considered adequate when > 95%. The tyrosinase and 2,2-diphenyl-1-picryl-hydrazyl-hydrate (DPPH) assays were performed in a 96-well plates Biotek Synergy HT plate reader, and read in the described wavelength. The compounds selected for the *ex vivo* testing were incorporated in a simple base comprised by Uniox C (cetearyl alcohol and polysorbate 60) at 0.1% (w/v) concentration. The base alone was also used as sham group.

2.2. Design of the compounds

The compounds were designed to explore the importance of each moiety in the *p*-coumaric acid's structure allied to an increased lipophilicity, which could help to achieve a better penetration in the skin than the prototype. Regarding this, ester, amide and ketone derivatives were prepared and tested in order to investigate whether these compounds are behaving as prodrugs or if they possess any activity *per se*. Different lengths of the alkyl chain were tested to explore the lipophilicity and potential hydrophobic interactions on the active site. Furthermore, the role of the phenol hydroxy group was also assessed through several phenolic compounds (such as **5–7**), since phenol group has radical scavenging activity that may chemically interfere with the oxidation process of tyrosinase over the substrate. Additionally, the phenolic pattern of the aromatic moiety seems to affect the inhibitory activity [9,22]. The set of compounds proposed are shown in Fig. 2.

2.3. Synthesis of the esters

The ester derivatives (**b-f**) were synthesized following classic Fischer esterification [18] using 1 mmol of the corresponding acid, 0.1 mL of concentrated sulfuric acid and the corresponding alcohol as solvent. The reaction proceeded for 3 h or until no more acid was observed in TLC. The reaction mixture was neutralized with aqueous $NaHCO_3$ saturated solution, and the solvent excess was evaporated under reduced pressure. The residue was taken up in 10 mL ethyl acetate and washed with 3x10 mL of saturated $NaHCO_3$ solution and 10 mL of water. The organic layer was dried with anhydrous Na_2SO_4. The desired compounds were further purified in a silica gel column chromatography, using hexane:ethyl acetate as eluent.

Methyl *p*-coumarate (**1b**). White solid (m.p. 134–136 °C); 57% yield. ^{1}H NMR ($CDCl_3$) δ 7.65 (d, J = 16.0 Hz, 1H), 7.42 (d, J = 8.6 Hz, 2H), 6.86 (d, J = 8.6 Hz, 2H), 6.30 (d, J = 16.0 Hz, 1H), 6.11 (s, 1H), 3.81 (s, 3H).

Ethyl *p*-coumarate (**1c**). Yellowish solid (m.p. 70–71 °C); 53% yield. ^{1}H NMR ($CDCl_3$) δ 7.56 (d, J = 16.0 Hz, 1H), 7.32 (d, J = 8.6 Hz, 2H), 6.99 (s, 1H), 6.80 (d, J = 8.6 Hz, 2H), 6.21 (d, J = 16.0 Hz, 1H), 4.19 (q, J = 7.1 Hz, 2H), 1.26 (t, J = 7.1 Hz, 3H).

n-Propyl *p*-coumarate (**1d**). Yellowish solid (m.p. 73–75 °C); 72% yield. ^{1}H NMR ($CDCl_3$) δ 7.64 (d, J = 16.0 Hz, 1H), 7.41 (d, J = 8.6 Hz, 2H), 6.88 (d, J = 8.6 Hz, 2H), 6.30 (d, J = 16.0 Hz, 1H), 4.17 (t, J = 6.7 Hz, 2H), 1.84 – 1.61 (m, 2H), 0.99 (t, J = 7.4 Hz, 3H).

i-Propyl *p*-coumarate (**1e**). Yellowish solid (m.p. 69–70 °C); 65% yield. ^{1}H NMR ($CDCl_3$) δ 7.62 (d, J = 15.9 Hz, 1H), 7.50 – 7.34 (m, 2H), 6.91 – 6.83 (m, 2H), 6.28 (d, J = 15.9 Hz, 1H), 5.14 (dt, J = 12.4, 6.2 Hz, 1H), 1.32 (d, J = 6.2 Hz, 6H).

n-Butyl *p*-coumarate (**1f**). Yellowish solid (m.p. 75–78 °C); 40% yield. ^{1}H NMR ($CDCl_3$) δ 7.63 (d, J = 16.0 Hz, 1H), 7.41 (d, J = 8.5 Hz, 2H), 6.85 (d, J = 8.5 Hz, 2H), 6.30 (d, J = 16.0 Hz, 1H), 4.21 (t, J = 6.6 Hz, 2H), 1.75 – 1.59 (m, 2H), 1.50 – 1.37 (m, 2H), 0.96 (t, J = 7.3 Hz, 3H).

Methyl cinnamate (**2b**). Yellowish oil; 59% yield. ^{1}H NMR ($CDCl_3$) δ 7.69 (d, J = 16.0 Hz, 1H), 7.59 – 7.44 (m, 2H), 7.44 – 7.28 (m, 3H), 6.44 (d, J = 16.0 Hz, 1H), 3.79 (s, 3H).

Ethyl cinnamate (**2c**). Yellowish oil; 57% yield. ^{1}H NMR ($CDCl_3$) δ 7.69 (d, J = 16.0 Hz, 1H), 7.57 – 7.46 (m, 2H), 7.41 – 7.36 (m, 3H), 6.44 (d, J = 16.0 Hz, 1H), 4.26 (q, J = 7.1 Hz, 2H), 1.33 (t, J = 7.1 Hz, 3H).

i-Propyl cinnamate (**2e**). Yellowish oil; 48% yield. ^{1}H NMR ($CDCl_3$) δ 7.67 (d, J = 16.0 Hz, 1H), 7.52 – 7.48 (m, 2H), 7.38 – 7.34 (m, 3H), 6.41 (d, J = 16.0 Hz, 1H), 5.14 (sept, J = 6.2 Hz, 1H), 1.31 (d, J = 6.2 Hz, 6H).

n-Butyl cinnamate (**2f**). Yellowish oil; 41% yield. ^{1}H NMR ($CDCl_3$) δ 7.68 (d, J = 16.0 Hz, 1H), 7.52 (dd, J = 6.6, 2.9 Hz, 2H), 7.45 – 7.33 (m, 3H), 6.44 (d, J = 16.0 Hz, 1H), 4.21 (t, J = 6.7 Hz, 2H), 1.78 – 1.61 (m, 2H), 1.54 – 1.34 (m, 2H), 0.97 (t, J = 7.4 Hz, 3H).

Methyl *p*-methoxycinnamate (**3b**). White solid (m.p. 85–86 °C); 77% yield. ^{1}H NMR ($CDCl_3$) δ 7.65 (d, J = 16.0 Hz, 1H), 7.47 (d, J = 8.7 Hz, 2H), 6.90 (d, J = 8.7 Hz, 2H), 6.31 (d, J = 16.0 Hz, 1H), 3.83 (s, 3H), 3.79 (s, 3H).

Ethyl *p*-methoxycinnamate (**3c**). Yellowish solid (m.p. 49–50 °C); 44% yield. ^{1}H NMR ($CDCl_3$) δ 7.64 (d, J = 16.0 Hz, 1H), 7.47 (d, J = 8.7 Hz, 2H), 6.89 (d, J = 8.8 Hz, 2H), 6.30 (d, J = 16.0 Hz, 1H), 4.25 (q, J = 7.1 Hz, 2H), 3.82 (s, 3H), 1.33 (t, J = 7.1 Hz, 3H).

Methyl caffeate (**4b**). White solid (m.p. 151–153 °C); 57% yield. ^{1}H NMR ($CDCl_3$) δ 7.59 (d, J = 15.9 Hz, 1H), 7.08 (d, J = 1.9 Hz, 1H), 7.01 (dd, J = 8.2, 1.9 Hz, 1H), 6.87 (d, J = 8.2 Hz, 1H), 6.27 (d, J = 15.9 Hz, 1H), 5.84 (br.s, 2H), 3.80 (s, 3H).

2.4. Synthesis of the amide 1g

The compound **1 g** was prepared following previous method described elsewhere [23]. In a flask 1.1 mmol of *p*-coumaric acid (**1a**), 1.1 mmol of 1-ethyl-3-(3-dimethylaminopropyl)carbodiimide (EDC) and 1.1 mmol of hydroxybenzotriazole (HOBt) hydrate were dissolved in 15 mL of dicloromethane. The mixture was stirred for 1 h, when 1 mmol of 1-butylamine was added. The reaction was carried out overnight and then washed with 2x10 mL 1 M HCl, 2x10 mL of saturated $NaHCO_3$ solution and 10 mL of water. The organic layer was separated, dried with anhydrous Na_2SO_4 and evaporated to give the pure product **1 g**.

N-Butyl-4-coumaramide (**1g**). White solid (m.p. 209–212 °C); 56% yield. ^{1}H- NMR (DMSO-d_6) δ 9.82 (s, 1H), 7.93 (t, J = 5.2 Hz, 1H), 7.38 (d, J = 8.5 Hz, 2H), 7.30 (d, J = 15.6 Hz, 1H), 6.78 (d, J = 8.5 Hz, 2H), 6.40 (d, J = 15.6 Hz, 1H), 3.15 (q, J = 6.0 Hz, 2H), 1.48 – 1.36 (m, 2H), 1.35 – 1.24 (m, 2H), 0.89 (t, J = 7.2 Hz, 3H). ^{13}C- NMR (DMSO-d_6) δ 165.71, 159.21, 138.89, 129.58, 126.50, 119.30, 116.18, 38.74, 31.80, 20.10, 14.15.

2.5. Synthesis of the ketones 1 h and 1i

The ketones were prepared following the previous report from our group [17,47]. Briefly, 1 mmol of 4-hydroxybenzaldehyde, and 1 mL of the corresponding ketone were dissolved in ethanol, and then 1 mL of 40% sodium hydroxide solution was added. The reaction proceeded for 24 h and after neutralization, ethanol was evaporated. The pure product was obtained by recrystallization from water.

1-(4-Hydroxyphenyl)but-1-en-3-one (**1h**). Yellowish solid (m.p. 109–112 °C); Yield 62%. ^{1}H NMR ($CDCl_3$) δ 7.55 – 7.36 (m, 3H), 6.87 (d, J = 8.7 Hz, 2H), 6.61 (d, J = 16.1 Hz, 1H), 5.55 (br. s, 1H), 2.37 (s, 3H).

1-(4-Hydroxyphenyl)hex-1-en-3-one (**1i**). Yellowish solid (m.p. 116–121 °C); Yield 68%. ^{1}H NMR ($CDCl_3$) δ 7.58 – 7.40 (m, 3H), 6.86 (d, J = 8.62 Hz, 2H), 6.63 (d, J = 16.1 Hz, 1H), 5.26 (br. s, 1H), 2.63 (t, J = 7.3 Hz, 2H), 1.81–1.61 (m, 2H), 0.98 (m, 3H).

2.6. Tyrosinase inhibition assay

The compounds were assessed for their tyrosinase inhibition activity on the monophenolase activity (when using L-tyrosine as substrate), following the previously described method elsewhere [9,15]. To these assays, the compounds were freshly prepared by dissolving them in phosphate buffer (50 mL KH_2PO_4 0.2 M + 11.5 mL NaOH 0.2 M, pH 6.5) with 0.1% DMSO to give a 1 mM stock solution. In a 96-well plate, 100 μL of each compound were transferred from the stock solution and serially diluted (50%) with phosphate buffer. After this, 50 μL of mushroom tyrosinase (~100 U/mL) were added and the solutions were incubated for 10 min at 25 °C. After this, 50 μL of 1.5 mM L-tyrosine solution were added to reach a final volume of 200 μL/well. The plate was immediately read at 490 nm wavelength and every 3 min during 30 min. Compound **1a**, a known tyrosinase inhibitor, was used as standard and phosphate buffer as negative control. The assay was performed in triplicate (n = 3), and the IC_{50} values were calculated by non-linear regression in the GraphPad Prism 6.0 software.

2.7. Antiradical activity

The antiradical activity of the compounds was assessed using the DPPH assay following the methodology described by Gaspar et al. [24]. Briefly, 100 μL of DPPH methanolic solution (250 μM) were added to a 96-well plate and afterward 100 μL of the stock solutions of the compounds (2 mM in methanol). The optical density (OD) from the plates were read for every 3 min until 30 min at 25 °C at 515 nm wavelenght. Methanol was used as negative control. The radical scavenging activity (%) was calculated by using the formulae 100 × [(control OD – sample OD) / control OD].

2.8. Docking studies

To simulate the *in silico* protein–ligand interaction the compounds were built in the software MarvinSketch 30.3 (ChemAxon Inc.) in a .mol format. The starting geometry was optimized subsequently through MM + molecular mechanics forcefield and semi-empirical PM3 method using the GaussView 5.0 software (Gaussian Inc.). GOLD software (CCDC, version 2020.1) was used for the docking simulations. The protein used was a mushroom tyrosinase (*Agaricus bisporus*) retrieved from the RCSB Protein Data Bank (PDB ID: 2Y9X) and the energy was minimized using the online server YASARA [25]. The binding site was defined as the atoms within 18 Å from the copper atoms in the active site. GoldScore and ChemPLP were used as scoring functions to predict the most likely binding pose of these compounds. The "allow early termination" default setting was deactivated and results with a maximal difference of 0.75 Å were clustered. The rest of the parameters were left on the default settings. Then, genetic algorithm was used to perform 100 docking runs for each compound. The highest scoring poses were considered for the evaluation of protein–ligand interactions, using a cut-off value of 4 Å for the interactions. Molecular interactions and visualization were done by using Discovery Studio Visualizer 20.1.0 (Dassault SystèmesBiovia Corp.).

2.9. Ex vivo efficacy assessment

The efficacy of the selected compounds **1a**, **1b**, **1c**, **1e** and **1f** was evaluated using the Fontana Masson methodology using human skin explants. These fragments were obtained from patients between 35 and 65 years old submitted to ophthalmic plastic surgery (Surgical Center of the Eye Bank of the Sorocaba Ophthalmological Hospital - BOS-HOS, Sorocaba-SP, Brazil), and kept in 0.9% saline buffer until the time of the experiment. The collection and use of these human skin explants derive from voluntary donation of the patient with their consent and approved by the Ethics Committee of the Hospital (HOS-BOS), and it is under the consubstantiate report number 3.065.484 registered in CONEP (National Committee of Research Ethics).

The samples were then immersed in 70% ethanol for 60 s for decontamination and rinsed twice in fresh saline buffer. The samples were cut on ~0.5 cm^2 fragments and transferred to a cell culture dish containing culture medium (Dulbecco's Modified Eagle Medium, DMEM, supplemented with 10% fetal bovine serum) leaving the skin to the top side without contact with the medium, for maintenance and nutrition of the tissue. The skin side of these fragments were immediately treated with the formulation of the compounds (base alone for sham group, no formulation for control group) and kept in contact with them for 72 h. During this period, the culture dish was maintained in a 95% humid atmosphere at 37 °C and 5% CO_2. The compounds were applied to the skin fragments at a rate of 12 mg/cm^2.

After the treatment, the fragments were fixed in 4% paraformaldehyde (pH 7.4) for 24 h and transferred to 30% saccharose solution for cryopreservation and inserted in tissue freezing medium. The samples were sectioned in 10 μm thickness slices in a cryostat (CN1850, Leica Biosystems) and directly collected onto silanized glass slides, where were stained by Fontana Masson technique [26].

2.10. Measument of the melanin content

Melanin content was measured by optical semi-quantitative method in the ImageJ software [27], adapting the guidelines proposed by Miot et al. [28]. Automatic segmentation of the pixels corresponding to the melanin of the other skin structures was used. In parallel, the selection of the black and white (B&W) color threshold, hue, saturation and brightness (HSB) color space and dark background were adjusted.

Afterwards, the selection of the area of interest for the quantification of melanin pigments was done from the viable epidermis using the freehand selection tool in the software. The pixels were semi-quantified using the measure function from the software. The average melanin content was normalized by the value of the selected area, and thus eventual variations in the thickness of the epidermis, according to the analyzed field, do not result in deviations from the evaluation.

2.11. ClogP estimation

The calculated *n*-octanol/water partition coefficient value was estimated using the calculator plugin from the Marvin software version 20.3.0 (ChemAxon Ltd.). The software uses a consensus method that weights the PhysProp data with the calculated logP (ClogP) using the Viswanadhan's method [29]. The electrolyte concentration for Na^+, K^+ and Cl^- used in the estimation was from default configuration (0.1 M).

2.12. Statistical analysis

The statistical analysis was carried out by analysis of variance (ANOVA). The Bonferroni's test was used for comparing the tested groups with the control group. The considered significance level was 95% ($p < 0.05$).

3. Results and discussion

3.1. Tyrosinase inhibition

Melanin overproduction may be caused by many different reasons,

leading to the darkening of the skin as a whole or in specific sites where the damage was made. This may lead to hyperpigmentation on the skin and melasma. Tyrosinase inhibitors are very useful in the treatment of such hyperpigmentations of the skin, especially if they show to be effective through topical administration. Therefore, promising compounds must have a good permeability to penetrate the skin and reach the melanocytes in the deepest epidermis layers.

Several tyrosinase inhibitors are already available for such purposes. Hydroquinone is chemically the 1,4-dihydroxybenzene and is widely used as a skin-whitening agent alone, or usually in combination with retinoids [4]. Arbutin, a glycosylated hydroquinone derivative, is also a tyrosinase inhibitor, but it is less associated to skin irritation and cytotoxicity related to hydroquinone [30]. Kojic acid is another natural product produced by fungi, such as *Penicillium* sp. and *Aspergillus* sp. This compound acts by chelating the copper ions present in the active site of tyrosinases and thus, inhibiting its activity [31,32]. The main problems related to these compounds are the safety, skin permeation issues (due to high hydrophilicity) and unwanted side effects.

The tested compounds showed inhibitory activity in micromolar range, which is compatible or even superior than other reports from literature [10,11,33]. The results presented in Table 1 indicate that the hydroxy group is very important to the activity, since its change by hydrogen (**2**) or methoxyl (**3**) led to considerable drop in the enzyme inhibition, leading to poorly active compounds. Although compound **4a** showed to be the less active acid, it was noted a quick darkening of the medium during the assay, suggesting that it may serve as a substrate on the diphenolase step (second step in Fig. 1) instead of a competitive inhibitor. Literature describes that **4a** is a covalent inhibitor of tyrosinase, since the enzyme can oxidize it to the corresponding *o*-caffeoquinone which is dark and a very reactive compound [34], explaining why it is also considered a suicide tyrosinase inhibitor. However, covalent inhibitors are frequently associated with severe side effects, such as allergies, tissue damage and carcinogenesis [35].

By definition, prodrugs should not possess biological activity; they should only serve as transport molecule of the active compound to the target tissue [36]. Accordingly, if the esters were to be prodrugs they should not have any inhibitory activity over the enzyme. However, the results from Table 1 show that the analogues **1b-f** were active inhibitors of the enzyme *per se* in the monophenolase step, with higher potencies than the prototype (**1a**). This is an interesting finding because the compounds not only could facilitate the permeation into the skin and produce higher efficacy as tyrosinase inhibitors, but also promote long lasting activity, since they will inevitably be hydrolyzed generating the acid **1a**, which is also an inhibitor. On the other hand, the esters from acids **2a**, **3a** and **4a** showed no relevant activity up to 1 mM, suggesting a unique ability from the coumaric esters to exhibit inhibitory activity and the essential role of the hydroxy group on this effect.

Table 1
Percentage of monophenolase activity at 1 mM (L-tyrosine as substrate) and IC_{50} of the tested compounds.

Compound	R	R'	% control (1 mM ± SEM)	pIC_{50} (± SEM)
1a	4-OH	OH	32 ± 2.6	3.52 ± 0.03
1b	4-OH	OMe	11 ± 1.3	4.02 ± 0.03
1c	4-OH	OEt	15 ± 2.4	4.01 ± 0.03
1d	4-OH	O^{n}Pr	10 ± 0.6	3.90 ± 0.02
1e	4-OH	O^{i}Pr	27 ± 2.7	3.66 ± 0.02
1f	4-OH	O^{n}Bu	< 10	4.16 ± 0.02
1 g	4-OH	NH^{n}Bu	22 ± 4.3	3.67 ± 0.04
1 h	4-OH	Me	27 ± 1.7	3.41 ± 0.03
1i	4-OH	^{n}Pr	16 ± 1.1	3.29 ± 0.03
2a	H	OH	52 ± 1.1	3.06 ± 0.04
2b	H	OMe	68 ± 5.5	< 3.00
2c	H	OEt	75 ± 7.4	< 3.00
2e	H	O^{i}Pr	87 ± 0.8	< 3.00
2f	H	O^{n}Bu	85 ± 2.8	< 3.00
3a	4-OMe	OH	56 ± 3.7	3.07 ± 0.06
3b	4-OMe	OMe	> 90	< 3.00
3c	4-OMe	OEt	70 ± 1.5	< 3.00
4a	3,4-diOH	OH	75 ± 3.6	< 3.00
4b	3,4-diOH	OMe	77 ± 3.2	< 3.00
5	3-OMe, 4-OH	–	74 ± 2.6	< 3.00
6	3-OMe, 4-OH	–	52 ± 2.9	3.11 ± 0.06
7	2-OH	–	19 ± 3.7	3.71 ± 0.04

It is noteworthy that the *p*-coumaric acid derivatives (**1**) possess a comparable or higher inhibitory effect on tyrosinase activity when compared to the prototype **1a**, and thus some SAR rules may be derived from this data. The methyl (**1b**) and ethyl (**1c**) derivatives have very similar IC_{50} values (~95 μM), which are 3-fold higher than the parent acid (296 μM). When increasing the length of the alkyl chain, the inhibitory activity improved considerably. The *n*-butyl ester compound **1f** is the most potent in the set, showing an IC_{50} value of 69 μM. This suggests that hydrophobic interactions in the binding site of the enzyme may occur, improving the affinity of such compounds. In counterpart, branching this chain seems negative contribution to the affinity. For instance, the *n*-propylic derivative **1d** (IC_{50} 124 μM) showed to be 2-fold more potent than the isopropylic ester **1e** (IC_{50} 221 μM). Similar findings were already observed with other phenolic acids such as orsellinates (2,4-dihydroxy-6-methyl benzoates), which had growing inhibitory activity when alkyl chains are elongated up to 8-carbon length [33].

Considering that the *p*-coumarate esters are active without the acid moiety, and the activity obtained with **1f**, the amide **1g** was also tested, considering the higher stability of this group. Additionally, non-hydrolysable analogues such as the ketones **1h** and **1i** were also evaluated. The results obtained with these compounds denote that the ester moiety is the best functional group to the interaction with the enzyme, since all presented lower affinity than the ester derivatives. The amide **1g** showed improved potency than the parent acid **1a**, with an IC_{50} value of 209 μM (1.4-fold higher). Regarding the ketones **1h** and **1i** the role of lipophilicity was different than in the esters, since the more lipophilic compound **1i** (IC_{50} 508 μM) showed decreased affinity than **1 h** (IC_{50} 386 μM). In summary, these results strongly suggest that both phenol and carboxylate moieties may perform favorable interactions with the enzyme, but also that the carboxylic acid is not essential to the interaction with tyrosinase, as suggested by the natural substrate, L-tyrosine.

In order to evaluate the role of the phenol group in the inhibitory effect on tyrosinase, simplified derivatives containing the phenolic moiety but lacking the carbonyl/carboxyl groups (**5**–**7**) were tested. These compounds showed inhibitory activity on tyrosinase with different degrees. The lower activity shown by eugenol (**5**) when compared to its isomer **6** suggests an important electronic effect given by the extended conjugation of the phenol group with the double bond, which is in line with previous reports [33]. In fact, non-conjugated analogues of *p*-coumaric acid were already tested, showing very low inhibitory activity on tyrosinase [9]. However, the increased potency of compound **7** in comparison to **5** and **6**, and also to **1a** denotes that the presence of the hydroxyl *ortho*-positioned in the aromatic ring is favourable to the interaction with the enzyme [16]. It has been demonstrated that both *ortho*- and *para*-phenolic compounds tend to have a better inhibitory activity than the *meta*-analogues, but the potency also depends on the remaining structural characteristics of the compounds [22].

3.2. Antiradical activity

It is widely known that phenols present radical scavenging activity that may also contribute totally or in part to the antimelanogenic effect of tyrosinase inhibitors. To investigate if the inhibitory activity observed for the compounds was due to an interaction with tyrosinase's active site or due to a redox effect, DPPH assay was performed with the compounds [37]. DPPH is a stable radical compound used to

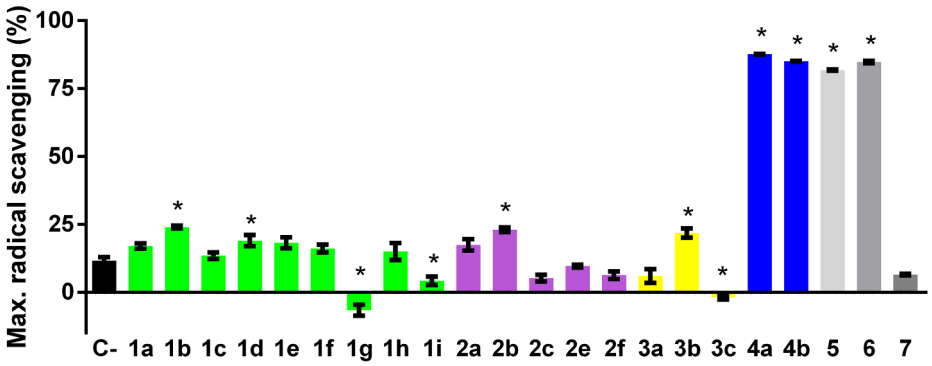

Fig. 3. Percentage of the maximum radical scavenging activity of the compounds in the DPPH assay. C- is the negative control (methanol). Black bars represent ± SEM. *$p < 0.05$ relative to the C-.

Table 2
Atoms or amino acid residues involved in the interactions with the ligands and respective measured distances, and the docking score for each studied compound.

Atoms / Residues	Type of interaction	Distance (Å)						
		tyrosine	1a	1b	1c	1d	1e	1f
Cu^{2+}	Coordinate bond	2.64	2.46	2.47	2.27	2.47	2.48	2.51
His84	Hydrogen bond	2.84	2.96	2.70	–	2.70	2.73	2.73
His60	Hydrogen bond	2.06	2.07	1.95	–	2.05	1.97	2.14
His295	Hydrogen bond	–	–	–	2.50	–	–	–
His262	π-π stacking	3.61	3.90	4.06	4.06	4.12	4.03	4.19
Val282	π-alkyl	4.14	4.00	3.00	2.99	2.95	3.02	2.79
Ala285	π-alkyl	4.54	4.77	5.20	5.21	5.31	5.19	5.38
Gly280	Hydrogen bond	2.44	–	–	–	–	–	–
Gly280	Hydrogen bond	2.63	–	–	–	–	–	–
Ser281	Hydrogen bond	–	2.54	–	–	–	–	–
Val247	Hydrophobic	–	–	5.07	5.06	5.00	4.30	5.32
Phe263	Hydrophobic	–	–	4.79	4.77	4.78	5.46	5.12
Met256	Hydrophobic	–	–	–	–	–	–	4.91
CHEMPLP Score		64.48	58.75	55.13	58.34	60.86	59.50	62.82

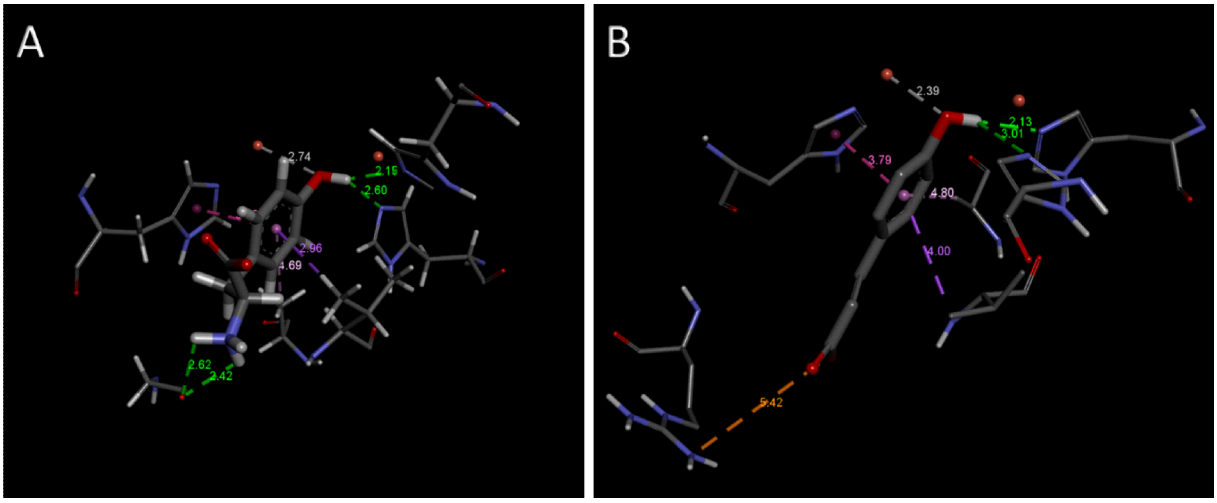

Fig. 4. Ligand interactions between L-tyrosine (A) and **1a** (B) and the amino acids in the active site of mushroom tyrosinase. Dashed lines represents the observed interactions. Green: hydrogen bond; purple: π-alkyl interactions; pink: π-π stacking; grey: coordinate bond. (For interpretation of the references to color in this figure legend, the reader is referred to the web version of this article.)

monitoring reactions involving radicals, which can be correlated to the antioxidant potential of tested compounds. DPPH presents a vibrant purple color that can be quantified by spectrophotometric method. In the presence of a radical scavenger, this compound is reduced to the corresponding hydrazine, which is a colorless or pale yellow compound. The difference in absorbance indicates the antiradical capacity of the tested compound [38]. Fig. 3 presents the results from the DPPH assay with the reported compounds.

As observed in the results, several compounds exhibited significant radical scavenging activity, and some other had strong DPPH scavenging activity such as the caffeates **4a** and **4b** (87.7 and 85.1%, respectively), and the phenolic compounds **5** and **6** (81.7 and 84.7%, respectively). This observation could be explained by the fact that the presence of an additional hydroxyl group (in comparison to *p*-coumaric acid) better stabilizes the phenoxyl radicals formed, prior to conversion to the corresponding quinone [9,39], and our results is also in line with

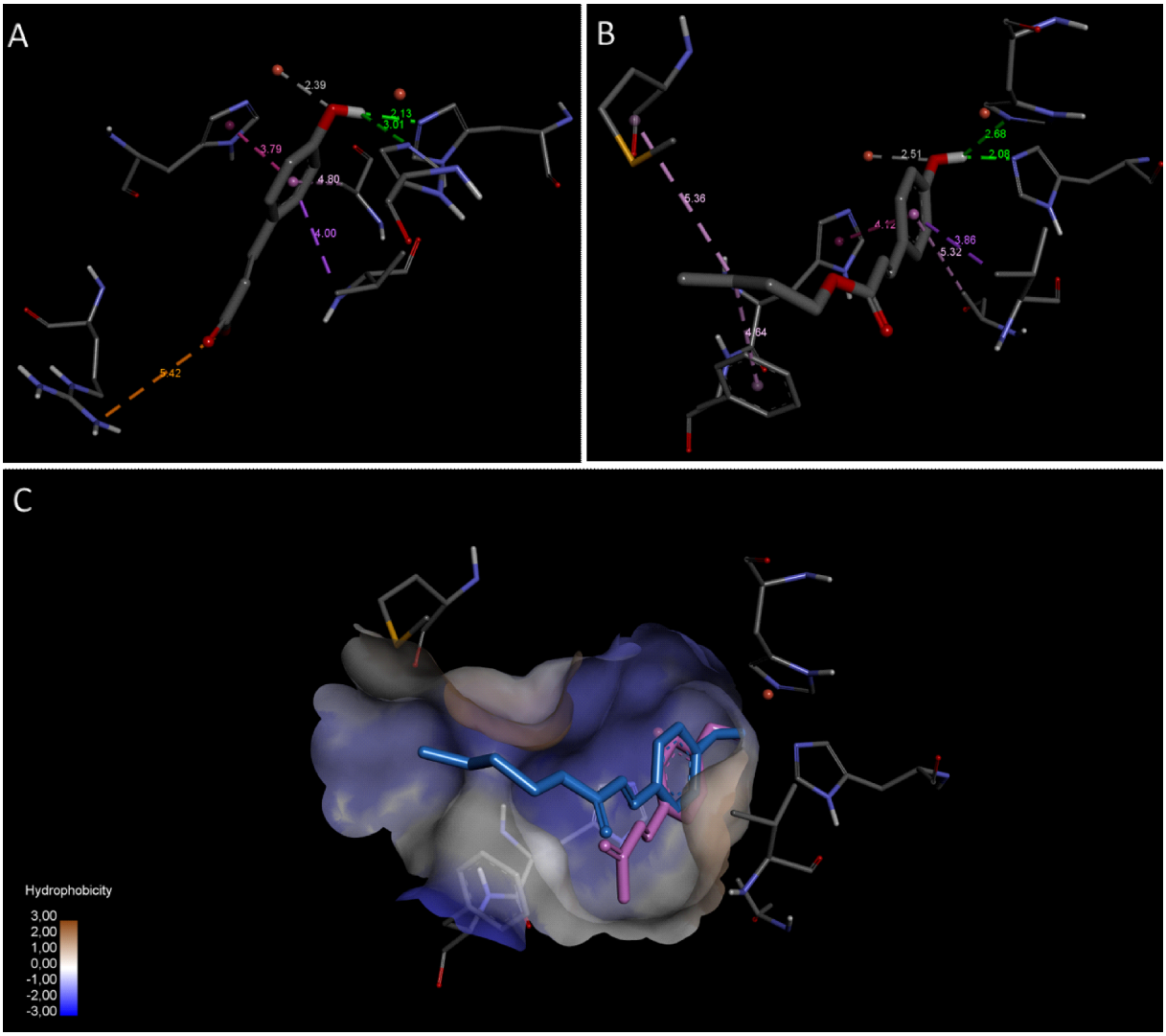

Fig. 5. Docking poses showing the hydrogen bonds of **1a** (A) and **1f** (B) with His60, His84 (dashed green lines), coordinate bond with copper atom (dashed grey lines), π-π stacking interactions (dashed pink lines) and π-alkyl interactions (purple dashed lines). (C) Hydrophobic potential surface of the binding site showing the fitting of the alkyl chain of **1f** (blue) into a hydrophobic pocket whereas the parent acid **1a** (purple) interacts with Arg267 in a more hydrophilic site. The hydrophobicity scale is shown, being the more hydrophobic site, the more red while the more hydrophilic site, the more blue. (For interpretation of the references to color in this figure legend, the reader is referred to the web version of this article.)

other literature reports [40].

Noteworthy, the other cinnamic acid derivatives, including *p*-coumaric acid, did not display any significant radical scavenging activity. This is in line with previous reports from literature [9]. However, Takahashi and Miyazawa [9] showed that the 2,3-dihydrocinnamates display stronger antiradical activity than the corresponding cinnamates. This suggests that the extended conjugation of the phenol hydroxyl reduces the radical scavenging effect. Moreover, the presence of electron-donating groups *ortho* or *para* to the phenol hydroxyl increases the radical scavenging activity, which explains the stronger effect of caffeates [9].

The report from Takahashi and and Miyazawa [9] clearly shows that the dihydrocinnamates are also less potent tyrosinase inhibitors than the corresponding cinnamates, being practically inactive. Our results, together with Takahashi and Miyazawa's [9] data, strongly suggests that the mechanism of tyrosinase inhibition for the compounds **1a-1i** are independent of a redox effect, since the more potent tyrosinase inhibition activity the less potent radical scavenging effect.

The results for the phenolic compounds **5–7** also shed light in this discussion. Eugenol (**5**) and isoeugenol (**6**) showed very strong antiradical activity. This is in line with previous literature reports for eugenol and isoeugenol in DPPH assays [41,42].

Interestingly, the position isomer 2-allylphenol **7** did not show significant antiradical activity, suggesting that the position of the hydroxy group in the ring strongly affects the activity. This lower activity may be due to the fact that compound **7** does not have the *ortho* methoxy group, as in both eugenol and isoeugenol, which may make it less capable of stabilizing the phenoxyl radical, or even due to the absence of an electron donating group in *para* position For instance, butylhydroxytoluene (BHT) is a known antioxidant which presents two *ortho t*-butyl groups and a *para* methyl group related to the hydroxyl [43].

Considering these aspects, it can be concluded that the observed tyrosinase inhibitory activity for the compounds **1a-i** is independent of an antioxidant effect, similarly to other reports from literature for other cinnamates [9].

3.3. Docking studies

To better understand how the compounds may interact with the catalytic site of mushroom tyrosinase, molecular docking studies were carried out. These studies were done with the compounds selected as more interesting. The highest scoring poses were chosen to investigate

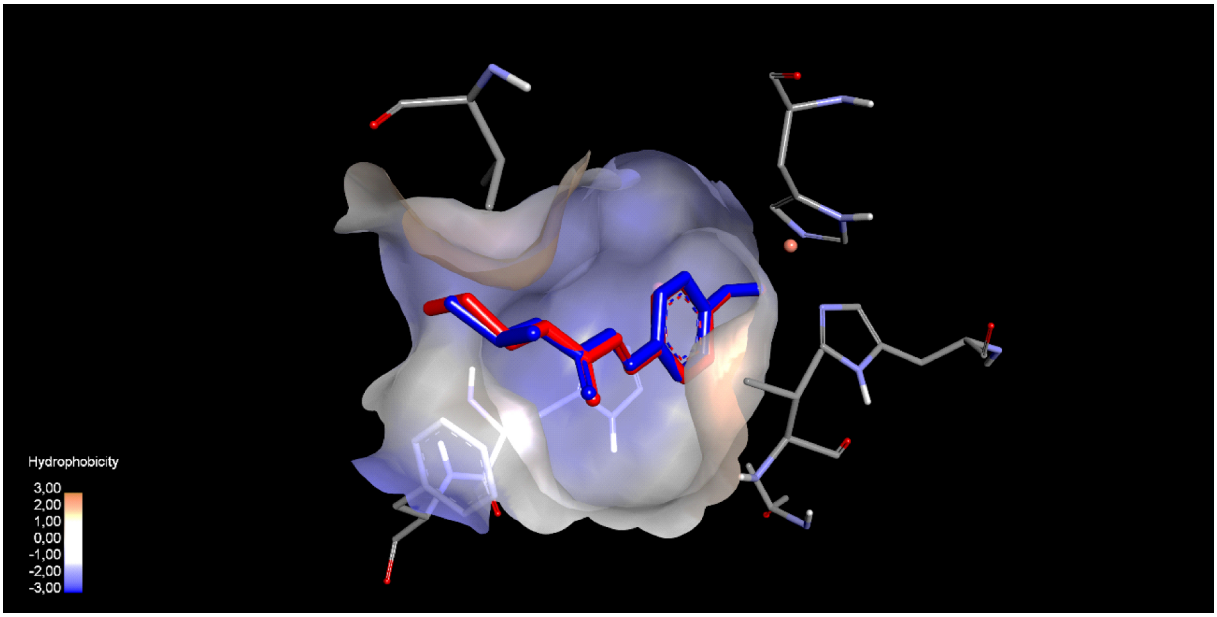

Fig. 6. Overlap of the isopropyl ester **1e** (blue) and *n*-propyl ester **1d** (red) in the binding site surrounded by a hydrophobic surface. The hydrophobicity scale is shown, being the more hydrophobic site, the more red while the more hydrophilic site, the more blue. (For interpretation of the references to color in this figure legend, the reader is referred to the web version of this article.)

the interactions between ligand and active site, and the summary of the interactions are presented in Table 2.

Compound **1a** interacts with the catalytic site in a similar manner as does L-tyrosine (Fig. 4), with the oxygen of the phenol ring coordinating to the copper ions and performing hydrogen bonds with the histidine residues His60 and His84. The protonated amino group from L-tyrosine seems to interact by hydrogen bonding with Gly281, and an additional hydrogen bond between the carbonyl group and Asn260 was also identified. Additionally, the negative charged carboxylate group of **1a** showed a salt bridge with the protonated guanidine group from Arg267 (Fig. 4B) and both ligands exhibit π-π stacking interactions with the histidines from the active site. These observed interactions are in line with other literature results from molecular docking [14,15,34,44].

The data from Table 2 clearly shows that the esters **1b-1f** perform additional hydrophobic interactions with the hydrophobic pocket comprised by the amino acids Val247, Phe263 and Met256 in the enzyme. These interactions thermodynamically contribute to better interaction with the target (as described by the CHEMPLP score), explaining why these compounds showed improved affinity to the enzyme than the acid prototype. Moreover, the esters seems to perform closer interactions with the Val282 and His84 residues. The remaining interactions seems very similar in the prototype and derivatives.

Docking analysis for the most active compound from the set, **1f**, showed similar interactions to the prototype **1a** with the amino acids His60 and His84 through hydrogen bonding, as well as the hydrophobic and π-π stacking interactions of the aromatic ring with Val282, Ala 285 and His262, respectively (Fig. 5A and B), which is also in line for similar compounds from literature [34]. However, due to the absence of the negatively charged carboxylate group, no interaction was observed with the Arg267 residue. On the other hand, the longer alkyl chain fits nicely into a hydrophobic pocket close to the catalytic site (Fig. 5C), comprised by the hydrophobic amino acids Met256 and Phe263, thus possibly conferring this analogue a higher activity than the prototype and also than the other less active esters. All these interactions provided the higher CHEMPLP score among the esters, and also corroborates the experimental data.

Interestingly, isopropyl ester **1e** showed about half of the potency compared to the *n*-propyl analogue **1d**, and the docking results are in line with the experimental data (Fig. 6). The isopropyl group from **1e** interacts with the hydrophobic amino acids in the same pocket, however the residues Val247 and Phe263 create a steric hindrance in the cavity, which hinders the adequate interaction of the isopropyl group as suggested by the distance values for these interactions. This seems to be the reason for the lower affinity of the isopropyl analogue **1e** in comparison to the non-branched analogue **1d**.

Overall, these modeling results suggest that the unsubstituted carboxylic acid is not essential to the activity of **1a**, and that the additional hydrophobic interactions provided by the alkyl chain from the esters play an important role in the affinity of such compounds. Although there is still some space for longer alkyl chains in the binding pocket, the excessive lipophilicity of such compounds limit their solubility in water and in the enzymatic assay medium. Therefore, the butyl ester **1f** was considered the optimal derivative for tyrosinase inhibitor in vitro.

3.4. Ex vivo efficacy assessment

Considering the potential of these compounds to be used as an active ingredient on formulations to hyperpigmentation treatment, the evaluation of their efficacy in human skin is necessary. Therefore, the prototype **1a** and some selected esters (**1b**, **1c**, **1e** and **1f**) were submitted to an *ex vivo* efficacy assay in order to evaluate the melanogenesis inhibition potential of these analogues.

This assay allows the evaluation of total depigmentation capacity of the tested compounds on human skin tissue [28]. Accordingly, the assay design allows the indirect evaluation of the permeability through the skin. The methodology uses ImageJ software to measure the melanin content per area through pixel analysis, which is compared to untreated control skin images. The higher pixel density indicates a higher melanin production. For this, evaluation, the compounds were applied at a test concentration of 0.1% (w/v).

The results are presented in Fig. 7, and clearly show that although **1a** is a known tyrosinase inhibitor, its efficacy was not observed in the performed assays. However, the esters **1c** and **1e** showed significant efficacy on reducing the melanin content in the skin fragments. This indicates that the analogues may present increased permeation through skin, and confirms their potential as antimelanogenic compounds by tyrosinase inhibition mechanism. Interestingly, compound **1e** showed the highest efficacy among the tested esters, although it is the less

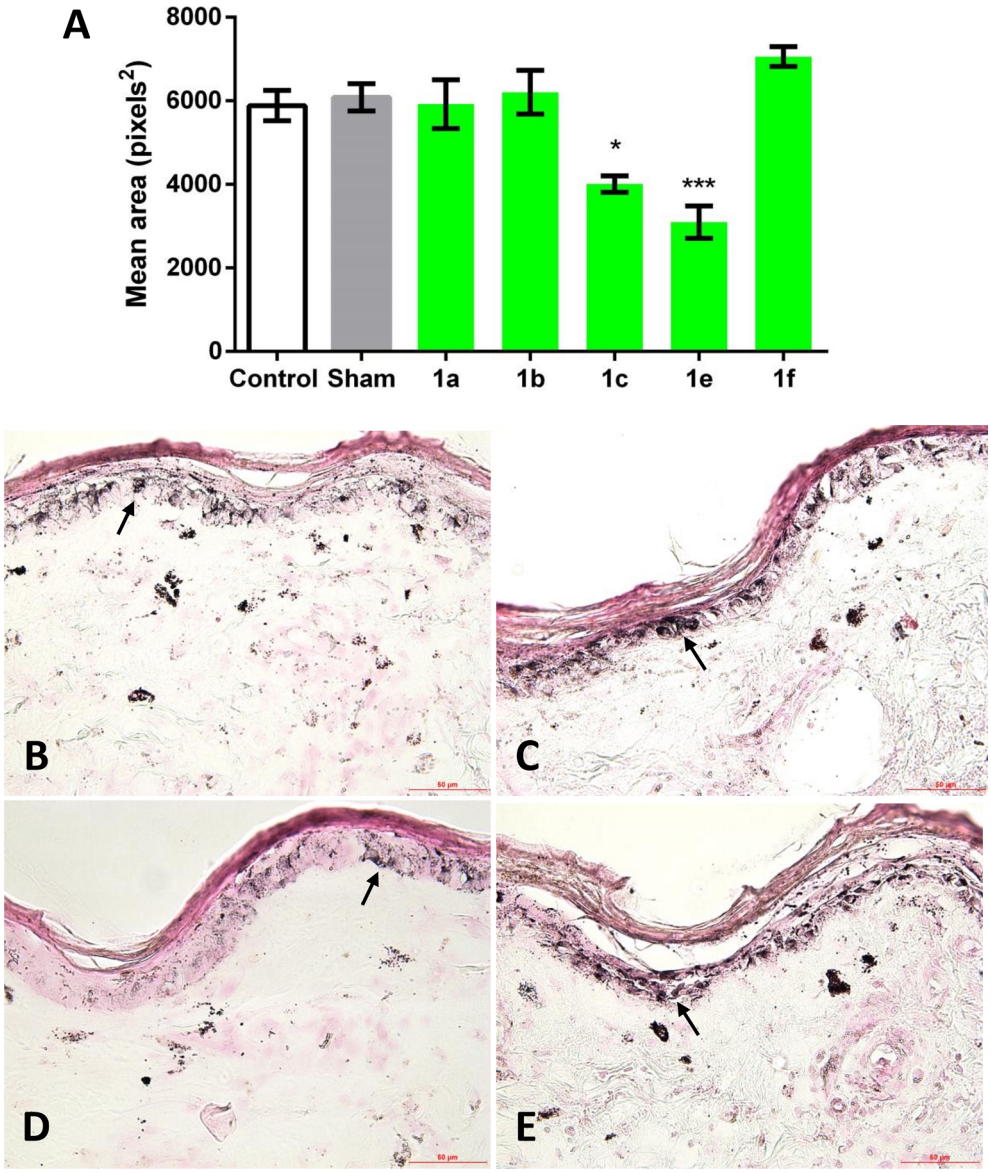

Fig. 7. (A) Melanin content measured in the *ex vivo* assay with the compounds. $*p < 0.05$; $***p < 0.001$ relative to the control. Sample micrographs obtained with the treatments with sham (B), **1a** (C), **1e** (D) and **1f** (E). The arrows indicate melanin deposits on the measured area. Note that compound **1e** produced less pigmented epidermis.

potent tyrosinase inhibitor. Moreover, the most potent compound from the series (**1f**) showed no efficacy on reducing the melanin content in the tested skin fragments. This suggests that the tyrosinase inhibitory activity should not be directly correlated to the efficacy in the skin.

There is no consensus in literature on which lipophilicity range (usually expressed by the calculated *n*-octanol/water partition coefficient value, ClogP) is adequate to good permeation through the skin, but it is accepted that molecules with moderate lipophilicity (ClogP 1–3) can diffuse through the skin [45,46]. Excessive lipophilicity may provide poor solubility and permeation issues accordingly, while low lipophilicity is not favorable to permeation through the hydrophobic layers of the epidemis and cell membranes. Moreover, low molecular weight (< 500) and low melting point are also favorable to adequate permeation [45]. Although *p*-coumaric acid **1a** present ClogP (1.83) value inside the expected range, it must be considered that it is predominantly deprotonated in the skin pH, and this ionized form presents ClogP −1.70, which explains its poor permeation through the skin.

On the other hand, the compounds presented herein are more lipophilic than the parent acid, and may better penetrate in the skin. Compound **1e** presents the highest ClogP value (2.99) inside the expected range, with lower melting point and the best efficacy in the *ex vivo* assays. Regarding this, possibly the most potent ester as tyrosinase inhibitor **1f** was ineffective due to excessive lipophilicity that may impair its penetration in the skin. This suggests that the balance between potency and lipophilicity must be considered when designing novel tyrosinase inhibitors

4. Conclusion

The results here presented showed that *p*-coumaric acid esters are effective antimelanogenic compounds with remarkable inhibitors of tyrosinase independent of radical scavenging activity. Docking studies indicate that the alkyl chain from these esters contributes to the affinity for the enzyme, but the lipophilicity balance with water solubility must be considered to design novel and more potent agents. Overall, these analogues should be considered for lead optimization to obtain effective compounds for hyperpigmentation topical treatment.

Declaration of Competing Interest

The authors declare that they have no known competing financial interests or personal relationships that could have appeared to influence the work reported in this paper.

Acknowledgements

The authors are grateful to the São Paulo Research Foundation – FAPESP for the financial support to JPSF working group (grant 2016/25028-3) and for the scholarship to MTV (grant 2018/03918-2), to the National Council for Scientific and Technological Development – CNPq for the scholarships to VGM and the fellowship to JPSF (grant 306355/2018-3) and to Coordination of Superior Level Staff Improvement – CAPES (financial code 001) for the scholarship to MF. Special thanks to Dr. Wagner Vidal Magalhães for the support to the Chemyunion team and to the contributions to this work, and to Dr. Daniela Rando for the tips in the molecular docking experiments.

Appendix A. Supplementary material

Supplementary data to this article can be found online at https://doi.org/10.1016/j.bioorg.2020.104108.

References

[1] S. Halaouli, M. Asther, K. Kruus, L. Guo, M. Hamdi, J.-C. Sigoillot, M. Asther, A. Lomascolo, Characterization of a new tyrosinase from Pycnoporus species with high potential for food technological applications, J. Appl. Microbiol. 98 (2005) 332–343, https://doi.org/10.1111/j.1365-2672.2004.02481.x.

[2] I. Polacheck, K.J. Kwon-Chung, Melanogenesis in cryptococcus neoformans, J. Gen. Microbiol. 134 (1988), https://doi.org/10.1099/00221287-134-4-1037.

[3] V. Ghodsinejad Kalahroudi, B. Kamalidehghan, A. Arasteh Kani, O. Aryani, M. Tondar, F. Ahmadipour, L.Y. Chung, M. Houshmand, Two novel tyrosinase (TYR) gene mutations with pathogenic impact on oculocutaneous albinism type 1 (OCA1), PLoS One. 9 (2014) e106656, , https://doi.org/10.1371/journal.pone.0106656.

[4] M. Chandra, J. Levitt, C. Pensabene, Hydroquinone therapy for post-inflammatory hyperpigmentation secondary to acne: not just prescribable by dermatologists, Acta Derm. Venereol. 92 (2012) 232–235, https://doi.org/10.2340/00015555-1225.

[5] Y.-J. Kim, H. Uyama, Tyrosinase inhibitors from natural and synthetic sources: structure, inhibition mechanism and perspective for the future, Cell. Mol. Life Sci. 62 (2005), https://doi.org/10.1007/s00018-005-5054-y.

[6] I. Kubo, K. Nihei, K. Tsujimoto, Methyl p-coumarate, a melanin formation inhibitor in B16 mouse melanoma cells, Bioorg. Med. Chem. 12 (2004) 5349–5354, https://doi.org/10.1016/j.bmc.2004.07.052.

[7] E.I. Solomon, U.M. Sundaram, T.E. Machonkin, Multicopper oxidases and oxygenases, Chem. Rev. 96 (1996) 2563–2606, https://doi.org/10.1021/cr9500460.

[8] K. Song, S.M. An, M. Kim, J.-S. Koh, Y.C. Boo, Comparison of the antimelanogenic effects of p-coumaric acid and its methyl ester and their skin permeabilities, J. Dermatol. Sci. 63 (2011) 17–22, https://doi.org/10.1016/j.jdermsci.2011.03.012.

[9] T. Takahashi, M. Miyazawa, Tyrosinase inhibitory activities of cinnamic acid analogues, Pharmazie. 65 (2010).

[10] Y.C. Boo, p-Coumaric acid as an active ingredient in cosmetics: a review focusing on its antimelanogenic effects, Antioxidants 8 (2019) 275, https://doi.org/10.3390/antiox8080275.

[11] S.M. An, J.-S. Koh, Y.C. Boo, p -coumaric acid not only inhibits human tyrosinase activity in vitro but also melanogenesis in cells exposed to UVB, Phyther. Res. (2010), https://doi.org/10.1002/ptr.3095.

[12] M.T. Varela, J.P.S. Fernandes, Natural products: key prototypes to drug discovery against neglected diseases caused by trypanosomatids, Curr. Med. Chem. 25 (2018), https://doi.org/10.2174/0929867325666180501102450.

[13] K. Pei, J. Ou, J. Huang, S. Ou, p -Coumaric acid and its conjugates: dietary sources, pharmacokinetic properties and biological activities, J. Sci. Food Agric. 96 (2016) 2952–2962, https://doi.org/10.1002/jsfa.7578.

[14] A. Garcia-Jimenez, J.L. Munoz-Munoz, F. García-Molina, J.A. Teruel-Puche, F. García-Cánovas, Spectrophotometric characterization of the action of tyrosinase on p -coumaric and caffeic acids: characteristics of o -caffeoquinone, J. Agric. Food Chem. 65 (2017) 3378–3386, https://doi.org/10.1021/acs.jafc.7b00446.

[15] Z. Sheng, S. Ge, X. Xu, Y. Zhang, P. Wu, K. Zhang, X. Xu, C. Li, D. Zhao, X. Tang, Design, synthesis and evaluation of cinnamic acid ester derivatives as mushroom tyrosinase inhibitors, Medchemcomm. 9 (2018) 853–861, https://doi.org/10.1039/C8MD00099A.

[16] A. Garcia-Jimenez, F. García-Molina, J.A. Teruel-Puche, A. Saura-Sanmartin, P.A. Garcia-Ruiz, A. Ortiz-Lopez, J.N. Rodríguez-López, F. Garcia-Canovas, J. Munoz-Munoz, Catalysis and inhibition of tyrosinase in the presence of cinnamic acid and some of its derivatives, Int. J. Biol. Macromol. 119 (2018) 548–554, https://doi.org/10.1016/j.ijbiomac.2018.07.173.

[17] M.T. Varela, M.M. Romaneli, M.L. Lima, S.E.T. Borborema, A.G. Tempone, J.P.S. Fernandes, Antiparasitic activity of new gibbilimbol analogues and SAR analysis through efficiency and statistical methods, Eur. J. Pharm. Sci. 122 (2018) 31–41, https://doi.org/10.1016/j.ejps.2018.06.023.

[18] F.A. Bernal, M. Kaiser, B. Wünsch, T.J. Schmidt, Structure-activity relationships of cinnamate ester analogues as potent antiprotozoal agents, ChemMedChem. 15 (2020) 68–78, https://doi.org/10.1002/cmdc.201900544.

[19] S. Omar, R. Abu-Reziq, Palladium Nanoparticles Supported on Magnetic Organic-Silica Hybrid Nanoparticles, J. Phys. Chem. C. 118 (2014) 30045–30056, https://doi.org/10.1021/jp510472t.

[20] A. Khatkar, A. Nanda, P. Kumar, B. Narasimhan, Synthesis, antimicrobial evaluation and QSAR studies of p-coumaric acid derivatives, Arab. J. Chem. 10 (2017) S3804–S3815, https://doi.org/10.1016/j.arabjc.2014.05.018.

[21] S.P. Lopes, Y.P. Castillo, M.L. Monteiro, R.R.P.P.B. de Menezes, R.N. Almeida, A.M.C. Martins, D.P. de Sousa, Trypanocidal mechanism of action and in silico studies of p-coumaric acid derivatives, Int. J. Mol. Sci. 20 (2019) 5916, https://doi.org/10.3390/ijms20235916.

[22] S. Ullah, C. Park, M. Ikram, D. Kang, S. Lee, J. Yang, Y. Park, S. Yoon, P. Chun, H.R. Moon, Tyrosinase inhibition and anti-melanin generation effect of cinnamamide analogues, Bioorg. Chem. 87 (2019) 43–55, https://doi.org/10.1016/j.bioorg.2019.03.001.

[23] L.C. Chan, B.G. Cox, Kinetics of amide formation through carbodiimide/ N- hydroxybenzotriazole (HOBt) couplings, J. Org. Chem. 72 (2007) 8863–8869, https://doi.org/10.1021/jo701558y.

[24] A. Gaspar, E.M. Garrido, M. Esteves, E. Quezada, N. Milhazes, J. Garrido, F. Borges, New insights into the antioxidant activity of hydroxycinnamic acids: synthesis and physicochemical characterization of novel halogenated derivatives, Eur. J. Med. Chem. 44 (2009) 2092–2099, https://doi.org/10.1016/j.ejmech.2008.10.027.

[25] E. Krieger, K. Joo, J. Lee, J. Lee, S. Raman, J. Thompson, M. Tyka, D. Baker, K. Karplus, Improving physical realism, stereochemistry, and side-chain accuracy in homology modeling: Four approaches that performed well in CASP8, Proteins Struct. Funct. Bioinforma. 77 (2009) 114–122, https://doi.org/10.1002/prot.22570.

[26] V.S. Carriel, J. Aneiros-Fernandez, S. Arias-Santiago, I.J. Garzón, M. Alaminos, A. Campos, A novel histochemical method for a simultaneous staining of melanin and collagen fibers, J. Histochem. Cytochem. 59 (2011) 270–277, https://doi.org/10.1369/0022155410398001.

[27] C.A. Schneider, W.S. Rasband, K.W. Eliceiri, NIH Image to ImageJ: 25 years of image analysis, Nat. Methods. 9 (2012) 671–675, https://doi.org/10.1038/nmeth.2089.

[28] H.A. Miot, G. Brianezi, A. de, A. Tamega, L.D.B. Miot, Techniques of digital image analysis for histological quantification of melanin, An. Bras. Dermatol. 87 (2012) 608–611, https://doi.org/10.1590/S0365-05962012000400014.

[29] V.N. Viswanadhan, A.K. Ghose, G.R. Revankar, R.K. Robins, Atomic physicochemical parameters for three dimensional structure directed quantitative structure-activity relationships. 4. Additional parameters for hydrophobic and dispersive interactions and their application for an automated superposition of certain, J. Chem. Inf. Model. 29 (1989) 163–172, https://doi.org/10.1021/ci00063a006.

[30] A.K. Chakraborty, Y. Funasaka, M. Komoto, M. Ichihashi, Effect of arbutin on melanogenic proteins in human melanocytes, Pigment Cell Res. 11 (1998) 206–212, https://doi.org/10.1111/j.1600-0749.1998.tb00731.x.

[31] M. Saeedi, M. Eslamifar, K. Khezri, Kojic acid applications in cosmetic and pharmaceutical preparations, Biomed. Pharmacother. 110 (2019) 582–593, https://doi.org/10.1016/j.biopha.2018.12.006.

[32] S. Kumari, S. Thng, N. Verma, H. Gautam, Melanogenesis inhibitors, Acta Derm. Venereol. 98 (2018) 924–931, https://doi.org/10.2340/00015555-3002.

[33] S. Zolghadri, A. Bahrami, M.T. Hassan Khan, J. Munoz-Munoz, F. Garcia-Molina, F. Garcia-Canovas, A.A. Saboury, A comprehensive review on tyrosinase inhibitors, J. Enzyme Inhib. Med. Chem. 34 (2019) 279–309, https://doi.org/10.1080/14756366.2018.1545767.

[34] A. Garcia-Jimenez, J.A. Teruel-Puche, P.A. Garcia-Ruiz, A. Saura-Sanmartin, J. Berna, J.N. Rodríguez-López, F. Garcia-Canovas, Action of tyrosinase on caffeic acid and its n-nonyl ester. Catalysis and suicide inactivation, Int. J. Biol. Macromol. 107 (2018) 2650–2659, https://doi.org/10.1016/j.ijbiomac.2017.10.151.

[35] R.A. Bauer, Covalent inhibitors in drug discovery: from accidental discoveries to avoided liabilities and designed therapies, Drug Discov. Today. 20 (2015) 1061–1073, https://doi.org/10.1016/j.drudis.2015.05.005.

[36] B.M.A. Sanches, E.I. Ferreira, Is prodrug design an approach to increase water solubility? Int. J. Pharm. 568 (2019) 118498, , https://doi.org/10.1016/j.ijpharm.2019.118498.

[37] İ. Gulcin, Antioxidants and antioxidant methods: an updated overview, Arch. Toxicol. 94 (2020) 651–715, https://doi.org/10.1007/s00204-020-02689-3.

[38] E.J. Garcia, T.L.C. Oldoni, S.M. de Alencar, A. Reis, A.D. Loguercio, R.H.M. Grande, Antioxidant activity by DPPH assay of potential solutions to be applied on bleached teeth, Braz. Dent. J. 23 (2012) 22–27, https://doi.org/10.1590/S0103-64402012000100004.

[39] J. Teixeira, A. Gaspar, E.M. Garrido, J. Garrido, F. Borges, Hydroxycinnamic acid antioxidants: an electrochemical overview, Biomed Res. Int. 2013 (2013) 1–11, https://doi.org/10.1155/2013/251754.

[40] I. Gulcin, Antioxidant activity of caffeic acid (3,4-dihydroxycinnamic acid), Toxicology. 217 (2006) 213–220, https://doi.org/10.1016/j.tox.2005.09.011.

[41] İ. Gülçin, Antioxidant activity of eugenol: a structure-activity relationship study, J. Med. Food. 14 (2011) 975–985, https://doi.org/10.1089/jmf.2010.0197.

[42] R. Bortolomeazzi, G. Verardo, A. Liessi, A. Callea, Formation of dehydrodiisoeugenol and dehydrodieugenol from the reaction of isoeugenol and eugenol

with DPPH radical and their role in the radical scavenging activity, Food Chem. 118 (2010) 256–265, https://doi.org/10.1016/j.foodchem.2009.04.115.
[43] İ. Gülçin, Antioxidant properties of resveratrol: A structure–activity insight, Innov. Food Sci. Emerg. Technol. 11 (2010) 210–218, https://doi.org/10.1016/j.ifset.2009.07.002.
[44] Y. Nazir, A. Saeed, M. Rafiq, S. Afzal, A. Ali, M. Latif, J. Zuegg, W.M. Hussein, C. Fercher, R.T. Barnard, M.A. Cooper, M.A.T. Blaskovich, Z. Ashraf, Z.M. Ziora, Hydroxyl substituted benzoic acid/cinnamic acid derivatives: Tyrosinase inhibitory kinetics, anti-melanogenic activity and molecular docking studies, Bioorg. Med. Chem. Lett. 30 (2020) 126722, , https://doi.org/10.1016/j.bmcl.2019.126722.
[45] K.B. Ita, Transdermal drug delivery: progress and challenges, J. Drug Deliv. Sci. Technol. 24 (2014) 245–250, https://doi.org/10.1016/S1773-2247(14)50041-X.
[46] J. Hadgraft, M.E. Lane, Skin permeation: the years of enlightenment, Int. J. Pharm. 305 (2005) 2–12, https://doi.org/10.1016/j.ijpharm.2005.07.014.
[47] Marina Varela, Thais A. Costa-Silva, João H.G. Lago, Andre G. Tempone, João Paulo S. Fernandes, Evaluation of the antitrypanosoma activity and SAR study of novel LINS03 derivatives, Bioorg. Chem. 89 (2019) 102996, https://doi.org/10.1016/j.bioorg.2019.102996.